sustainability

MDPI

Article

Stiffening and Toughening of Asphalt Mastic Induced by Bitumen–Mineral Selective Molecular Adsorption and Nanostructural Reconstruction

Zhiyang Liu [1,*], Haipeng Wang [2], Xiangbing Gong [3], Peng Cui [4] and Hongrui Wei [5]

[1] College of Civil and Transportation Engineering, Shenzhen University, Shenzhen 518061, China
[2] Sichuan Highway Planning, Survey, Design and Research Institute Ltd., Chengdu 610041, China
[3] State Engineering Laboratory of Highway Maintenance Technology, Changsha University of Science & Technology, Changsha 410114, China
[4] Beijing Urban Construction & Development Group Co., Ltd., Beijing 100045, China
[5] School of Transportation Engineering, Shandong Jianzhu University, Jinan 250101, China
* Correspondence: liuzhiyang@szu.edu.cn

Abstract: Asphalt mastic is the most important binder in asphalt mixtures and its rheology is inevitably influenced by the mineral aggregates. Due to the little consideration that has been paid to aggregates' effects, the rheological properties of mastic films have not been accurately characterized for the present method. Therefore, this study aimed to investigate the rheological characteristics of mastic affected by mineral aggregates and reveal its fundamental mechanism of interfacial interaction. The results suggest that the aggregates increased the stiffness and toughness of mastic within the linear and nonlinear viscoelastic regions. The mastic on limestone had a higher linear viscoelastic modulus than that on basalt below 35 °C, and its ratio reached up to 1.18. However, the modulus of the mastic on basalt surpassed that on limestone by over 50 °C, and the maximum ratio reached 2.17. The mastic in contact with the limestone had a higher failure strain and failure modulus than that in contact with the basalt, the ratios of which reached 1.60 and 1.32, respectively. The macrorheological characteristics are closely related to the nanostructures and intermolecular interactions of bitumen–mineral systems. The coexistence of a stable bitumen nanostructure and an adsorbed layer on the calcite substrate provided a strong bonding energy and high resistance to external shear deformation, leading to the high stiffness and toughness of the limestone. Abundant metal ions from augite and albite diffused into the bitumen layer and destroyed its nanostructure, decreasing the stability of the mastic–basalt interface system. The non-bond energy of bitumen-calcite was 14.15% higher than that of bitumen-albite, and the ratio of shear stress of the bitumen-calcite to the bitumen-albite reached up to 6.8. Therefore, the calcite in limestone reinforced the bitumen, and the augite and albite in basalt destroyed the bitumen colloidal structure. This provides a fundamental understanding of the rheological characterization of mastic on mineral aggregates.

Keywords: asphalt mastics; rheology; mineral aggregates; nanostructure; molecular dynamics

Citation: Liu, Z.; Wang, H.; Gong, X.; Cui, P.; Wei, H. Stiffening and Toughening of Asphalt Mastic Induced by Bitumen–Mineral Selective Molecular Adsorption and Nanostructural Reconstruction. *Sustainability* **2023**, *15*, 4398. https://doi.org/10.3390/su15054398

Academic Editors: Ruxin Jing, Peng Wang, Xianyong Ma and Xiaorui Zhang

Received: 1 February 2023
Revised: 22 February 2023
Accepted: 28 February 2023
Published: 1 March 2023

1. Introduction

Asphalt mastic is one of the most important components in asphalt mixtures and has been long known to influence asphalt mixture design, construction, and performance [1–7]. Asphalt mastic is regarded as the real bonding agent that cements mineral aggregates in an asphalt mixture [8], and the stiffness and tackiness of the mastic make essential contributions to the bearing capacity and durability of the asphalt mixture. The physico-chemical interactions between the polar components of the bitumen and the active sites of the aggregates' surfaces influence the molecular arrangement of the bitumen within several nanometers near the mineral aggregates, which changes the rheological properties of the mastic film in contact with the aggregates.

Asphalt mastic is composed of bitumen and fillers passed through a no. 200 sieve [9], and the rheological behavior of asphalt mastics on mineral surfaces is characterized by more complicated interactions relative to bulk mastics, as can be seen in Figure 1. In the mastic–aggregate interfacial transition region, the rheological behavior of the mastic film is mainly affected by the bitumen–aggregate interaction and the filler–aggregate interaction. The bitumen–aggregate interaction is mainly attributed to the reconstruction of the nano- and microstructure of bitumen driven by the intermolecular energy from the mineral ions or groups. The reoriented structure of bitumen near the minerals is a distinct response to the external oscillating load, which manifests different rheological properties at a macroscale. On the other hand, compared with bulk mastic, the filler particles in a mastic film with a thickness of a few millimeters or hundreds of microns have a markedly higher possibility of contact with each other and the aggregate surface with close gaps, thus leading to a higher proportion of the bitumen film being dominated by the bitumen aggregates. Therefore, the presence of these two interactions leads to the rheological differences between bulk mastics and mastic films near the aggregates.

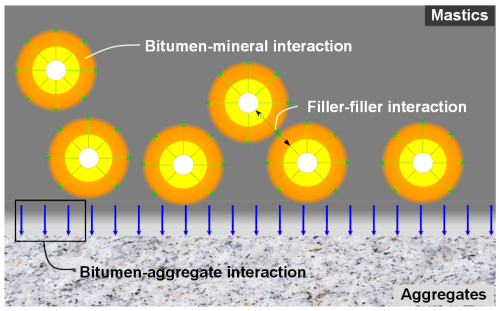

Figure 1. Intercomponent interactions of the mastic–aggregate interface.

Considerable work has focused on the rheology of bulk asphalt mastics. Some of the early work by Rigden [10] investigated the relationships between mastic flow properties and various filler concentrations. Craus and coworkers [2] conducted a comprehensive investigation into the micromechanics of asphalt mastic and summarized some key factors, including surface area, texture, activity, and selective sorption. The rheology of asphalt mastics has been extensively studied due to the good correlation with real construction. Using the SHRP program for testing bitumen, the rheological and failure properties of mastic were investigated in depth [11–13]. Anderson and coworkers [11] found that the rheological properties of mastic approximately satisfy the time–temperature superposition principle, which provides a valid approach to effectively analyze the rheology in a wide frequency range. They also concluded that the rheology of mastic depends highly on the filler mineralogy. This indicates the important impact of mineralogy on mastic properties. Buttlar demonstrated that the rheological properties of bulk mastic are dominated by bitumen–filler or bitumen–mineral interactions [3], and many micromechanical models have been proposed [3,14–18]. Kumlai observed that the filler type has a more significant influence on asphalt mastic's rheological properties than the bitumen type [19]. The wettability and physicochemical properties of the mastic is closely related to the lithology of the filler [20]. These studies support the good prediction of bulk mastic mechanical properties when neglecting the effects of surface mineralogy.

Compared with bulk asphalt mastics, mastics on a mineral surface undergo not only filler–bitumen and filler–filler interactions but also bitumen–aggregate and filler–aggregate interactions, so mastics may have distinct rheological behavior. Limited studies on the effects of surface mineralogy on mastic rheology have been reported. Research on the rheological properties of bitumen on diverse mineral surfaces can provide some beneficial insights. Scholz and Huang [21,22] studied the rheology of bitumen on different mineral surfaces and found significant impacts on mineralogy. Cho and Bahia [23] also observed differences in rheological parameters with different aggregates when studying moisture

damage to the bitumen–aggregate interface. Xu demonstrated that adhesion depends on aggregate mineralogy and has a negative correlation with moisture damage [20]. Zhang observed different moduli of asphalt mastics containing limestone, basalt, and granite fillers [24]. Huang detected different morphologies of interfacial transition zones depending on mineralogy [25]. The mineralogy of the aggregate's surface affects bitumen–aggregate and filler–aggregate interactions and further alters the rheological behavior of mastics. In a real mixture, the interface of asphalt mastics and mineral aggregates is an important component, and the rheological characteristics of mastics on mineral surfaces highly affect the overall performance of the mixture. Investigation into the effects of diverse mineral surfaces could support a comprehensive understanding of mixtures' mechanical behaviors.

Molecular dynamics is an effective tool for directly simulating molecular interactions between bitumen and mineral aggregates [26–29]. It fundamentally calculates the intermolecular and intramolecular forces and potential energy, and also numerically solves Newton's equations of motion for a molecular system. Molecular dynamics has been employed to investigate bitumen–aggregate interaction and adsorption [30]. The spatial and temporal variations and movements of the material's molecular compounds and the internal energy dissipation can be readily investigated from the trajectories. It can provide more fundamental and intuitive insight into the nanostructural evolution and intermolecular interaction of bitumen affected by mineral aggregates.

The rheological characteristics of asphalt mastic in a real asphalt mixture are significantly affected by the mineral aggregates. Therefore, the objective of this study was to investigate the rheological properties of mastic in contact with various mineral aggregates and to reveal their internal micromechanisms driven by intermolecular interactions using molecular dynamics following the flowchart in Figure 2. At a macrolevel, the linear rheological properties of mastic on limestone, basalt, and original steel plates were tested by frequency sweep tests, and their nonlinear viscoelasticities on various substrates were measured by strain sweep tests. At a molecular level, molecular models of the "sandwich" layer interface combining bitumen and primary minerals in the aggregates were established. The nanostructural evolution, bitumen–mineral interaction, and nanomechanical properties were investigated from the molecular trajectory. A multiscale relationship between macrorheology and nanomolecular behavior is elaborated. This could promote the accurate rheological characterization of mastic in the field and provide a fundamental understanding of the rheological behavior affected by the bitumen–mineral interaction.

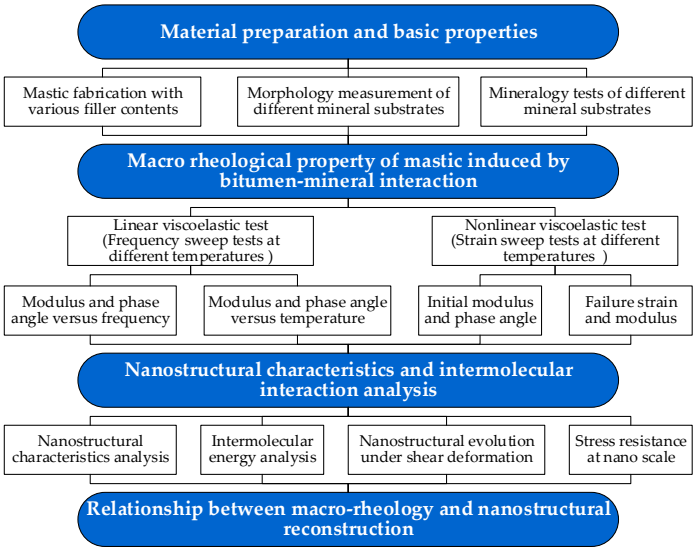

Figure 2. Flowchart of this study.

2. Materials and Methods

2.1. Materials and Sample Preparation

2.1.1. Bitumen and Asphalt Mastic

An 80/100 penetration-grade bitumen from Karamay and limestone filler passed through a no. 200 sieve were used to fabricate asphalt mastic. The basic physical properties of the bitumen and filler were tested and met the requirements of the Technical Specifications for Construction of Highway Asphalt Pavements (JTG F40-2004) [31]. The bitumen and limestone filler were preheated at 165 °C for 4 h to obtain a liquid uniform bitumen. The filler was equally divided into several portions and was successively mixed into the hot bitumen using a high-shear homogenizer at a speed of 1500 rpm at 165 °C. The mixed asphalt mastic was mildly stirred at 200 rpm at 165 °C until it reached a uniform state. Generally, the mass ratio of filler and bitumen in a field asphalt mixture varies from 0.8 to 1.2. Three asphalt mastics with mass ratios of 0.9, 1.0, and 1.1 were prepared following the same process.

2.1.2. Mineral Substrates

Three different substrates, including the original steel plate of the rheometer (ST), a limestone substrate (LS), and a basalt substrate (BS), were selected as the contacting surfaces. The chemistry, mineralogy, and roughness of the substrates may affect the rheological behavior of the contacting asphalt mastic. This study emphasizes the rheological characteristics of asphalt mastic affected by the chemical or mineral composition. Thereby, to eliminate the influence of the roughness, the mineral substrates were polished until a similar roughness to the original steel substrate of the rheometer was obtained. The morphologies of the three substrates were probed using a laser confocal microscope, and their roughness was calculated, as seen in Figure 3. This showed that the limestone and basalt substrates had smooth surfaces with a roughness of 0.15 µm and 0.19 µm, respectively, which are of the same order of magnitude and even lower than that of the original steel substrate. Therefore, the effect of such low roughness on the rheology of the mastic could be assumed to be negligible.

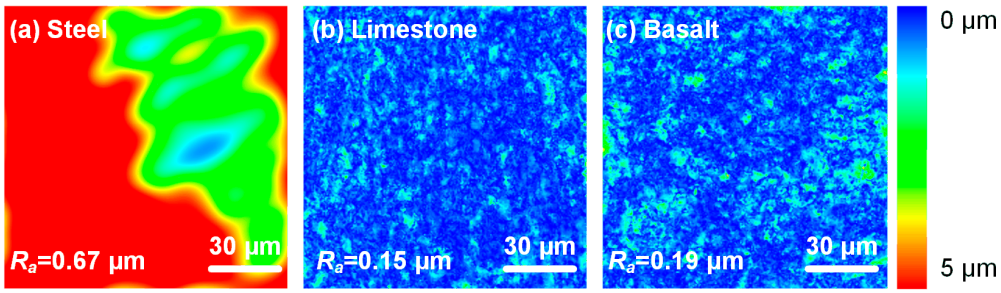

Figure 3. Morphologies of the mineral substrates.

The primary oxide amounts in the mineral substrates were measured by X-ray fluorescence spectrometry, as detailed in Table 1. These results suggested that limestone has abundant calcium oxide and that its mass concentration reaches 94.84%. However, basalt has a complex oxide composition, including 51.55% SiO_2, 16.38% Al_2O_3, 9.77% MgO, 7.73% Fe_2O_3, 5.29% CaO, and 4.89% Na_2O, indicating plentiful aluminosilicate with Mg, Fe, Ca, and Na. Considering the general mineral composition of limestone and basalt, the minerals in the substrates were determined by matching elemental compositions, as summarized in Table 1. Limestone is mainly composed of calcite, whereas basalt contains 28.82% anorthite, 23.36% augite, and 47.83% albite.

Table 1. Chemical and mineral compositions of the limestone and basalt substrates.

Oxide Mass Concentration (%)			Primary Mineral Composition (%)			
	Limestone	Basalt	Limestone		Basalt	
SiO_2	2.5	51.55	Calcite ($CaCO_3$)	100	Anorthite ($CaAl_2Si_2O_8$)	28.82
CaO	94.84	5.29				
Al_2O_3	1.21	16.38				
MgO	0.42	9.77			Augite ($Mg_6Fe_6Si_8O_{28}$)	23.36
Fe_2O_3	0.44	7.73				
Na_2O	0.05	4.89			Albite ($NaAlSi_3O_8$)	47.83
Other	0.55	4.4				

2.2. Rheological Characteristic Tests

The traditional rheological test was modified by substituting the original steel substrate in contact with different mineral substrates. The limestone and basalt substrates were cored and incised into cylindrical disks with 80 mm diameters for rheological tests below 35 °C and 200 mm diameters for tests over 35 °C. The cored aggregate disks were bonded to the upper and bottom plates of the dynamic shear rheometer using epoxy. The nonlinear viscoelastic (NLVE) response of the asphalt mastic was investigated by strain sweep and stress sweep tests. The strain sweep test measures the dynamic complex modulus of asphalt mastic by applying various strains at a constant temperature and frequency, whereas the stress sweep test investigates the complex modulus under different stresses. The modulus of asphalt mastic generally decreases with the increase in applied strain and stress, but the stress–strain relationship in strain and stress sweep tests may exhibit significant differences. Figure 4 displays the stress–strain relationship of the asphalt mastic with a 1.1 filler–bitumen ratio in the stress and strain sweep tests. The strain sweep test is more concerned with mechanical responses than the stress sweep test and is better for analyzing the effects of diverse contacting plates, which was also observed in previous research [2]. Therefore, the strain sweep test was preferred to investigate the nonlinear rheological behavior rather than the stress sweep test.

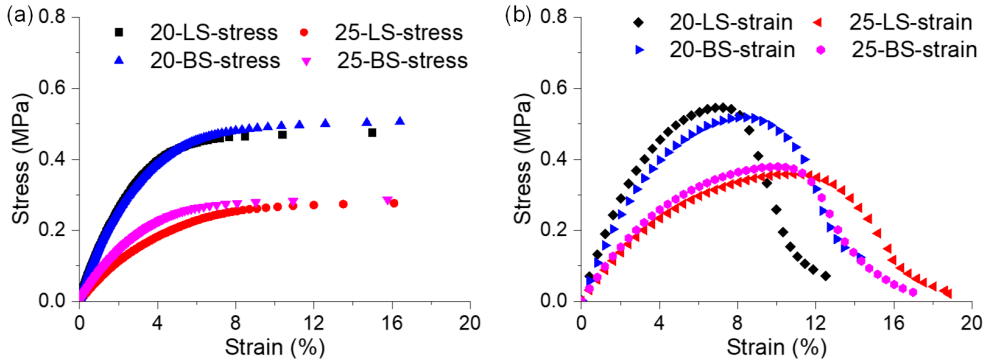

Figure 4. Stress–strain relationships in the stress and strain sweeps of mastics with a 1.1 filler–bitumen ratio on limestone and basalt substrates. (**a**,**b**) are the stress-strain curves in the stress sweep and strain sweep tests, respectively.

Strain sweep tests at a strain ranging from 0.0005% to 200% at 20 °C and 25 °C and 10 Hz were conducted to investigate the nonlinear viscoelastic responses of asphalt mastic in contact with various mineral substrates. The strain limit of the linear viscoelastic (LVE) region is defined as the strain at which the modulus decreases to 95% of the initial value, which was determined by the results of strain sweep tests. The frequency sweep tests of asphalt mastic in contact with diverse plates were conducted by applying strain in the LVE region at a frequency range from 0.1 Hz to 50 Hz at 5–80 °C. The linear and nonlinear rheological properties of the asphalt mastic on the three different substrates were compared and analyzed.

2.3. Molecular Dynamics Simulation

2.3.1. Molecular Models

Bitumen–mineral "sandwich" molecular models were established to explain the fundamental mechanism of the interaction between bitumen and mineral aggregates at a molecular level. A ternary bitumen system, containing 12.52 wt.% asphaltene, 16.45 wt.% resin, and 71.03 wt.% saturates, was selected, and it was verified by comparing the predicted and measured properties in a previous study [32]. For the substrates, we chose the primary minerals in the limestone and basalt substrates, including calcite, anorthite, augite, and albite. The periodic bitumen–mineral systems were assembled with mineral and bitumen layers, as seen in Figure 5.

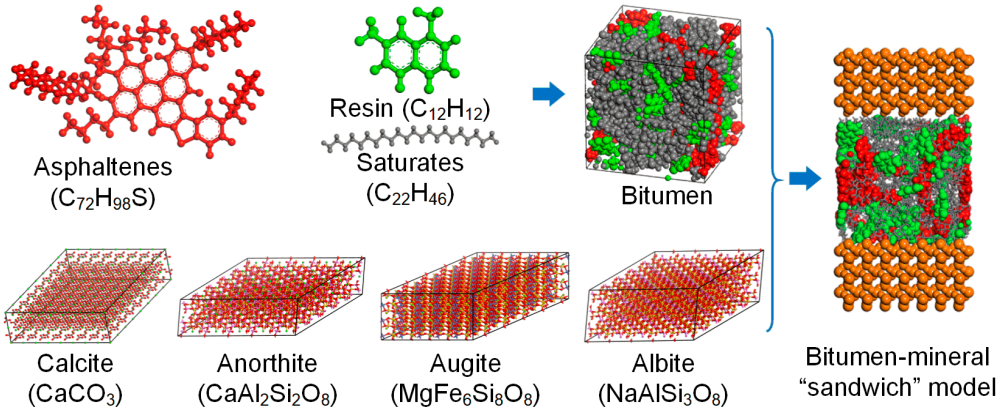

Figure 5. Bitumen–mineral "sandwich" molecular models.

2.3.2. Molecular Dynamics

The third generation of the Condensed-Phase Optimized Molecular Potentials for Atomistic Simulation Studies forcefield (COMPASS III) was utilized to calculate the energies of the systems. Geometric optimization, annealing, and molecular dynamics (MD) simulation at a constant temperature and volume (NVT) ensemble were performed to equilibrate the system. After the convergence of the total energy, the equilibrated systems underwent MD for 1 ns with a time step of 1 fs at the NVT ensemble of 298 K. Subsequently, a mineral substrate shearing simulation at 0.2 Å/ps at the NVT ensemble of 298 K was performed to investigate the molecular arrangements, structures, and mechanical properties.

3. Results and Discussion

3.1. Linear Rheological Characteristics of Asphalt Mastic in Contact with Various Mineral Aggregates

Frequency sweep tests of mastics on diverse plates with a small strain applied in the LVE region were conducted to investigate the relations between rheological properties and angular frequency and temperature. The complex moduli ratios and phase-angle ratios of mastics on mineral aggregates to steel plate at various frequencies and temperatures were determined to analyze the influence of aggregates on mastic stiffness in the LVE region.

3.1.1. Modulus Analysis at Various Frequencies

The complex modulus ratios of asphalt mastics on the mineral aggregates to the original steel plate were calculated and are plotted in Figure 6. Almost all the modulus ratios of the mineral aggregates decreased with increased frequency; however, their initial values and slopes significantly depended on the temperature, the mastic's filler–bitumen ratio, and the mineral aggregates. The mastic with a 0.9 filler–bitumen ratio in contact with the limestone substrate had a decreased modulus ratio with an increase in temperature. In contrast, the modulus ratio of the mastic on the basalt substrate at 50 °C was much higher than that at 20 °C. This indicates a significant distinction between the influences of limestone and basalt substrates on mastic rheology. The high temperature is likely to

stiffen the mastic on the basalt substrate but soften the mastic on the limestone substrate, which may be ascribed to the different chemical and mineral compositions of limestone and basalt. The mastic with a 1.1 filler–bitumen ratio exhibited similar temperature- and substrate-dependence. As the temperature rose, the modulus ratio of the mastic with a 1.1 filler–bitumen ratio on the limestone substrate decreased, while the modulus ratio of the mastic on the basalt substrate increased. The main difference between the mastic with a filler–bitumen ratio of 0.9 and that with a ratio of 1.1 was that the mastic with a higher filler content exhibited less variation in response to changes in temperature. High concentrations of filler in the mastic may weaken the physicochemical interactions between mastic and mineral aggregates.

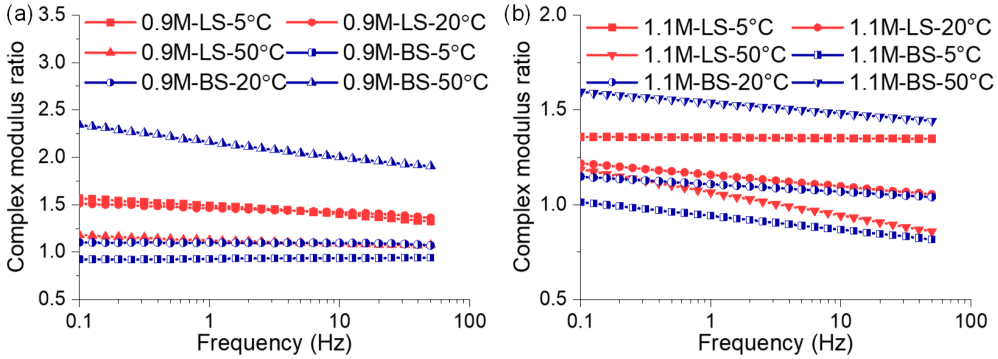

Figure 6. The complex modulus ratios of asphalt mastics on mineral aggregates to the original steel plate at different temperatures and frequencies, including the mastics with (**a**) 0.9 and (**b**) 1.1 filler–bitumen ratios.

The phase-angle ratio of the mastic on the mineral aggregates to the steel plate is depicted in Figure 7. The phase-angle ratios almost decreased with increased frequency and increased with rising temperature. However, the mastics with various filler amounts on the different substrates had different phase-angle ratios. The mastic with a certain filler dosage on the limestone substrate exhibited a lower phase-angle ratio than that on the basalt substrate at the same temperature and frequency. The mastic on the basalt substrate likely presented a larger viscous component in the mastic's rheological behavior than that on the limestone substrate, which is related to the chemical difference between basalt and limestone. Compared with the mastic with different filler–bitumen ratios in Figure 7a,b, a high-content filler in mastic weakens the variation in the phase-angle ratio in response to changes in temperature and frequency.

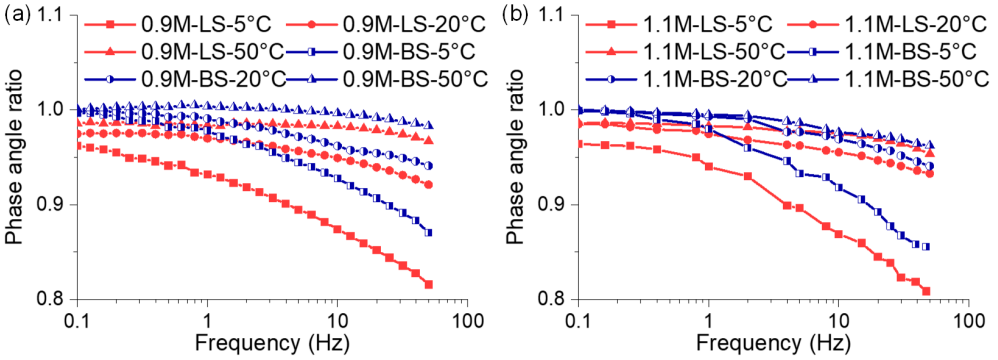

Figure 7. The phase-angle ratios of asphalt mastics on mineral aggregates to the original steel plate at different temperatures and frequencies, including the mastics with (**a**) 0.9 and (**b**) 1.1 filler–bitumen ratio.

3.1.2. Modulus Analysis at Different Temperatures

To compare the effects of mineral substrates at various temperatures, the complex modulus and phase-angle ratios against temperature are presented in Figure 8. At a temperature below 35 °C, the modulus ratios of part mastics on mineral substrates were

lower than one, indicating a softening action of the mineral aggregates compared with the steel plate. However, as the temperature exceeded 35 °C, the modulus ratios of mastics on mineral aggregates were greater than one and increased with rising temperature. This suggests that the mineral aggregates harden the mastic with respect to steel plates, and the hardening impact was enhanced by the high temperature. Moreover, the mastics on the basalt substrate had a slightly lower modulus ratio than those on the limestone substrate at a low temperature, which is consistent with the observed results in previous studies [21–23]. However, at temperatures above 35 °C, the modulus ratio of the mastic on the basalt substrate exceeded that of the mastic on the limestone substrate and increased rapidly with rising temperature. This implies that, at low temperatures, the limestone has a stronger interaction with the mastic than the basalt substrate. This is generally attributed to strong interaction between the active sites in limestone and bitumen polar components. Limestone contains abundant calcite with numerous active ions on the surface that generate strong electrostatic interaction at low temperatures [23]. Although the high temperature strengthened the interaction between mastic and limestone and basalt, the growth rate of the basalt–bitumen interaction with rising temperature was much higher than that of the limestone–bitumen interaction. Accordingly, the basalt substrate interacts with the bitumen more strongly than the limestone substrate at high temperatures. Additionally, the mastic on the limestone substrate has a lower phase-angle ratio than that on the basalt substrate. This indicates that the mastic on the limestone substrate presents a more viscous behavior than that on the basalt substrate. Some minerals in the limestone substrate may enhance the viscosity of the mastic but weaken its elasticity with respect to the basalt substrate [24]. The chemical and mineral compositions of the limestone and basalt substrates could be the major contributors to the linear viscoelastic behaviors of the mastics on the mineral aggregates [20].

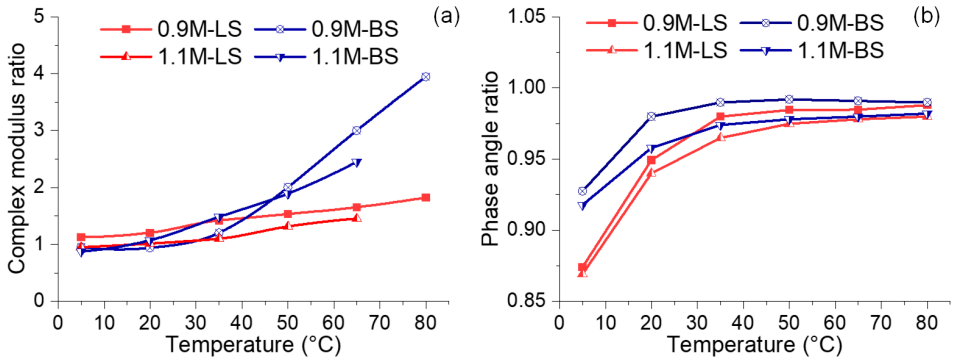

Figure 8. The rheological properties of mastics with various filler–bitumen ratios on mineral surfaces to the steel plate at different temperatures and 10 Hz including (**a**) complex modulus ratio and (**b**) phase-angle ratio.

3.2. Nonlinear Rheological Properties of Asphalt Mastics Affected by the Mineral Aggregates

3.2.1. Nonlinear Rheological Characterization of the Mastic

The strain sweep test investigates the rheological behavior of mastic in response to increased strain, and the complex modulus and phase angle variation with the applied strain can be obtained based on the measured oscillatory stress and strain. To characterize the nonlinear rheological properties of mastic, several parameters, including initial modulus, initial phase angle, failure modulus, and failure phase angle, have been proposed. The initial modulus and initial phase angle are defined as the complex modulus and phase angle of the mastic with 0.01% strain applied, as shown in Figure 9b, which describes the stiffness and response hysteresis at minor strain. The failure point is defined as the stress peak point in the stress–strain curve of the strain sweep, as presented in Figure 9a, at which the slope of the modulus–strain curve makes the transition from the increase stage to the decrease stage, as seen in Figure 9b. This means that the rate of modulus reduction changes

to decrease from an increase at the failure point. The failure strain and modulus describe the maximum strain and modulus before mechanical damage.

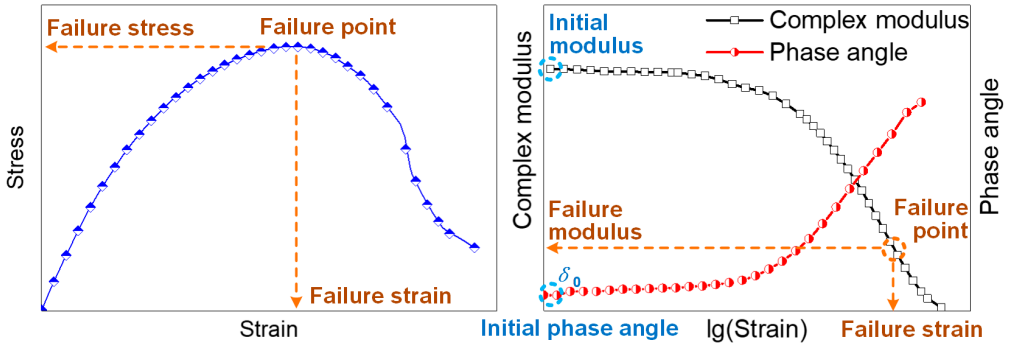

Figure 9. Diagram of nonlinear rheological properties based on the strain sweep test.

3.2.2. Initial Modulus and Phase Angle of Mastic on Different Mineral Substrates

The phase angles and complex moduli of mastics on diverse plates when a small strain was applied (0.01%) are shown in Figure 10. Overall, the initial phase angles and moduli of mastics on the mineral aggregates differed from the results for the steel plate. At both 20 °C and 25 °C, the mastic on the limestone substrate had the highest initial modulus, followed by the one on the basalt substrate, while the lowest modulus was recorded for the steel plate. Both at 20 °C and 25 °C, the mastic on the limestone substrate had the highest initial modulus, that on the basalt substrate had the second highest, and that on the steel plate had the lowest. This indicates that the mastics on the mineral aggregates are stiffer than those on the steel plate. Likewise, the initial phase angle of the mastic on the limestone aggregates was the lowest, followed by that of the mastic on the basalt, and that of the mastic on the steel was the highest. This suggests that the mineral aggregates enhanced the storage modulus and weakened the viscous nature of the mastic. The interaction between asphalt and aggregates may produce a rigid absorbed binder layer in the mastic–aggregate interface, the absorbed binder layer strengthening the mastic stiffness and diminishing the viscous rheological response. A thicker absorbed binder layer in the mastic–limestone interface due to their higher affinity leads to more notable impacts than in the case of basalt. Consequently, aggregate surfaces improve the elastic modulus of mastic when a small strain is applied.

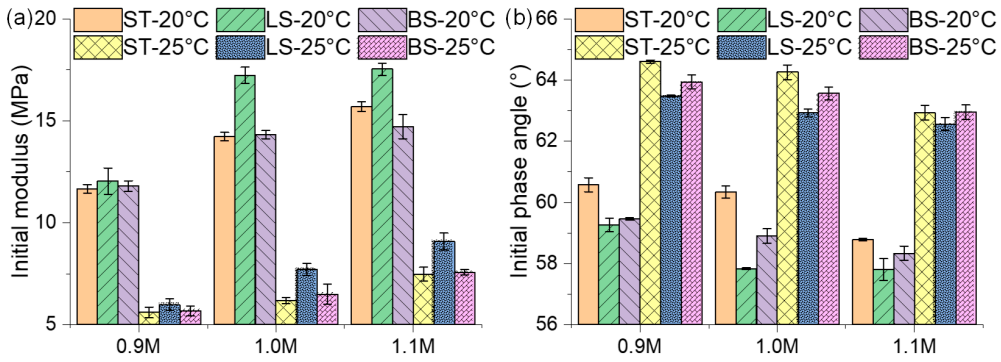

Figure 10. Initial moduli and phase angles of asphalt mastics on different mineral substrates in the strain sweep test at 20 °C and 25 °C. (**a**) is the initial modulus and (**b**) is the initial phase angle.

3.2.3. Failure Strain and Failure Modulus of Mastic on Different Mineral Substrates

The failure strain and modulus are, respectively, the strain and modulus at the peak point of a stress–strain curve in a strain sweep test, which characterizes the mechanical failure properties of the NLVE region. When the applied strain exceeds the failure strain, the decrease in the stress response indicates the occurrence of plastic deformation and

internal damage in mastic. The modulus reduction rate begins to slow down beyond the load capacity. As shown in Figure 11, the failure strains of the mastics on mineral aggregates decreased and the corresponding moduli slightly rose compared with the mastic on the steel plate. Failure strain reduction implies a decrease in mastic toughness, and modulus elevation strengthens the stiffness of the mastic. The ultimate impacts of aggregate surfaces are roughly equivalent to aggravating material brittleness. The mastic on the limestone substrate had a higher failure modulus and lower failure strain than that on the basalt substrate, indicating that the mastic on the limestone substrate is tougher than that on the basalt substrate. The interaction between bitumen and substrates induced by the chemistry and minerals of the aggregates may be attributed to the rheological differences between the mastics on the mineral aggregates and on the steel plate. Limestone was demonstrated to have a better affinity with bitumen than basalt in previous studies [20,24]. Calcite in limestone is widely acknowledged to be basic and probably chemically interacts with the acid anhydride in bitumen from considerable macrophenomena [20]. Explicit chemical production of bitumen–aggregate reactions has been controversial [24]. However, what is certain is that the active components in bitumen and aggregates generate physical attraction and adsorption [3,28]. More in-depth investigations into bitumen–mineral interactions at a molecular level are needed.

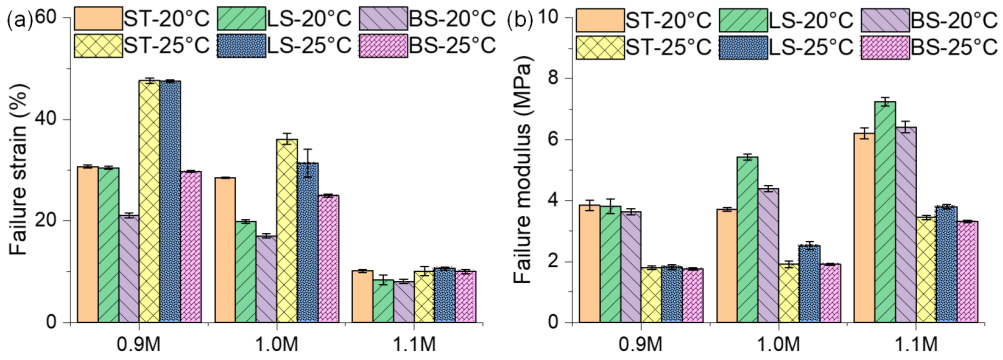

Figure 11. Failure strains and moduli of asphalt mastics on different mineral substrates in the strain sweep test at 20 °C and 25 °C. (**a**) is the failure strain, and (**b**) is the failure modulus.

3.3. Nanostructural Characteristics and Intermolecular Interaction Analysis between the Bitumen and Minerals

The equilibrated nanostructures of the bitumen–mineral interface systems are the synthetic result of the intermolecular and intramolecular interactions of bitumen and mineral molecules. The nanostructure of the bitumen in contact with different mineral substrates was predicted by molecular dynamics and is presented in Figure 12. The original colloidal structure of the bitumen was restructured due to the bitumen–mineral interaction; thereby, molecules with a strong polarity and low steric hindrance, such as resin, are adsorbed on the surface of the mineral substrates. The large asphaltene molecules with many condensed aromatic rings hardly overcome the hindrance from other bitumen molecules; thus, the main plane of asphaltene condensed rings is crowed from the adsorbed layer on the mineral surface. Moreover, the metal ions in the mineral substrates, including Mg^{2+} in the augite and Na^{+} in the albite, diffuse into the colloidal structure of the bitumen layer and produce a strong electrostatic interaction with the bitumen molecules. The Mg^{2+} in the augite have a roughly uniform dispersion in the bitumen layer, whereas the Na^{+} in the albite only surround the asphaltene micelles. In contrast, the Ca^{2+} in the calcite and anorthite are rigorously constrained by the anions in the minerals and do not penetrate the bitumen layer. However, the Ca^{2+} and CO_3^{2-} in the calcite produce a strong interaction with the polar bitumen molecules, including the abundant resin and even the whole asphaltene aromatic plane.

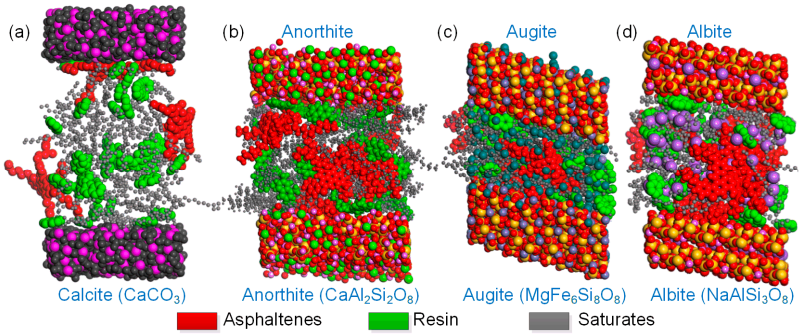

Figure 12. Molecular configurations of bitumen–mineral interface systems including (**a**) bitumen-calcite system, (**b**) bitumen-anorthite system, (**c**) bitumen-augite system and (**d**) bitumen-albite system.

The intermolecular interaction between bitumen and minerals is the intrinsic driving force for the formation of the bitumen nanostructure. The components of the intermolecular interaction are shown in Figure 13 and suggest a strong dependence on the minerals in the substrates. Overall, the minimum total non-bond energy appears in the bitumen–anorthite interface system, followed by the bitumen–calcite and bitumen–albite systems, and the total non-bond energy between bitumen and augite even has a positive value. A negative non-bond energy indicates intermolecular attraction; conversely, a positive value means intermolecular repulsion. Therefore, the anorthite in the basalt benefits the bitumen–aggregate adhesion, but the augite impairs the interfacial adhesion. The total non-bond energy is a sum of van de Waals, electrostatic, and long-range terms, and the van de Waals energy is the main contribution of the non-bond energy between the bitumen and mineral. The bitumen–anorthite system has a comparable van de Waals energy but a much higher electrostatic energy than the bitumen–calcite system; thus, the bitumen presents a slightly higher non-bonded energy with the anorthite than the calcite. The aluminum atoms in the anorthite present an amphoteric chemical nature and provide more electrostatic energy with the bitumen compared with the calcite. The relatively low van de Waals and electrostatic energies of the bitumen–albite system lead to its low non-bonded energy. Compared with the anorthite, the albite has a similar chemical composition but a much lower non-bonded energy, indicating that the Ca^{2+} exhibits a much stronger interaction with the bitumen molecules than the Na^{+}. Unexpectedly, bitumen–augite has a positive van de Waals energy, the solute value of which even exceeds the sum of the negative electrostatic and long-range energies. The positive van de Waals energy may be related to the dispersed Mg^{2+} and strong interaction between the top and bottom augite substrates, as seen in Figure 12. This results in a small gap between the top and bottom augite substrates and a much tighter arrangement of bitumen molecules. According to the Lennard–Jones intermolecular potential [33], when the distance between the non-bonding particles is smaller than the van der Waals radius, the intermolecular force presents repulsion. Consequently, the tight molecular arrangement results in the repulsive intermolecular force between Mg^{2+} and bitumen molecules and positive van de Waals energy. On the other hand, the dispersed Mg^{2+} in the bitumen layer causes a strong electrostatic action but cannot offset the van de Waals repulsion. Therefore, the bitumen–augite system has a low and positive non-bonded energy.

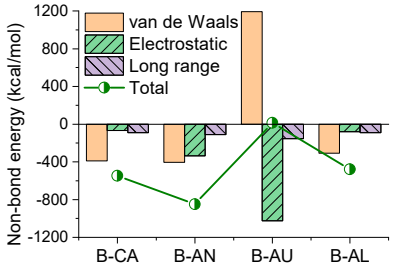

Figure 13. Bonding energy of the equilibrated bitumen–mineral system.

3.4. Nanomechanical Characteristics of the Bitumen–Mineral Interface under Shearing Displacement

The nanostructural evolution of the bitumen colloidal system attached to the mineral aggregates significantly influences the dynamic response under shear loading. The nanostructures of the various bitumen–mineral systems under 2 nm shear deformation are plotted in Figure 14. The bitumen–calcite and bitumen–anorthite systems have similar nanostructures with adsorbed polar bitumen molecules on the substrate surface, dissociated bitumen colloid, and stretched but clinging linear saturates. The dispersed metal ions in the bitumen layers of the bitumen–augite and bitumen–albite systems undergo strong intermolecular interactions with the polar groups in the bitumen. Accordingly, the diffused metal ions selectively adsorb the bitumen molecules simultaneously with strong polarity and low steric hindrance from the original bitumen colloidal structure, which cripples the bitumen colloid and weakens the association of bitumen molecules. The loose bitumen presents a weak resistance to the external shear. Moreover, the colloidal micelles composed of the diffused ions and small polar bitumen molecules have a low steric hindrance and rapid deformation relaxation, which further decreases the shear stress under shear deformation. In particular, the Na^+ in the bitumen layer near the albite substrates seem to form a shearing interface between the adsorbed bitumen and bulk bitumen.

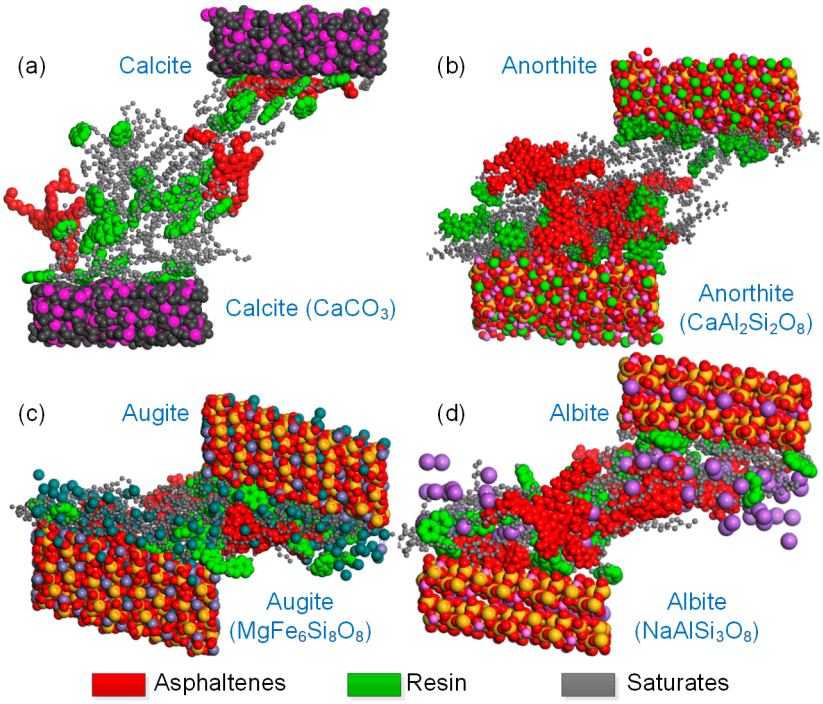

Figure 14. Molecular configuration of bitumen–mineral systems under 2 nm shear deformation including (**a**) bitumen-calcite system, (**b**) bitumen-anorthite system, (**c**) bitumen-augite system and (**d**) bitumen-albite system.

The rheological behavior is the macrodynamic response of mastic at a macroscale under oscillatory loading; likewise, the different bitumen–mineral systems present different dynamic responses at a molecular scale under shearing loading applied to the substrates. The shear stress of the bitumen–mineral systems is the synthetic result of the nanostructural evolution, bitumen molecular potential, and bitumen–mineral interaction, and is summarized in Figure 15. Overall, the shear stress τ_{yx} exhibited the most significant fluctuation, whereas the other shear stresses varied relatively slightly near zero in all the bitumen–mineral systems. However, the amplitude τ_{yx} in the bitumen–calcite and bitumen–anorthite systems was much higher than in the bitumen–augite and bitumen–albite systems. In the bitumen–calcite and bitumen–anorthite systems, the shear stress τ_{yx} had a significantly higher wave followed by a series of fluctuating peaks in each cycle, which was attributed

to the periodical tearing and reconstruction of the bitumen colloid during shearing. The destruction of the bitumen colloidal system consumed considerable external work and generated a strong resistance to the substrate shearing, leading to the marked stress wave. In contrast, the bitumen nanostructure with the dispersed metal ions in the bitumen–augite and bitumen–albite systems impaired the integrity and stability of the original colloid and weakened the resistance to the substrate shearing, resulting in a relatively small shear variation amplitude.

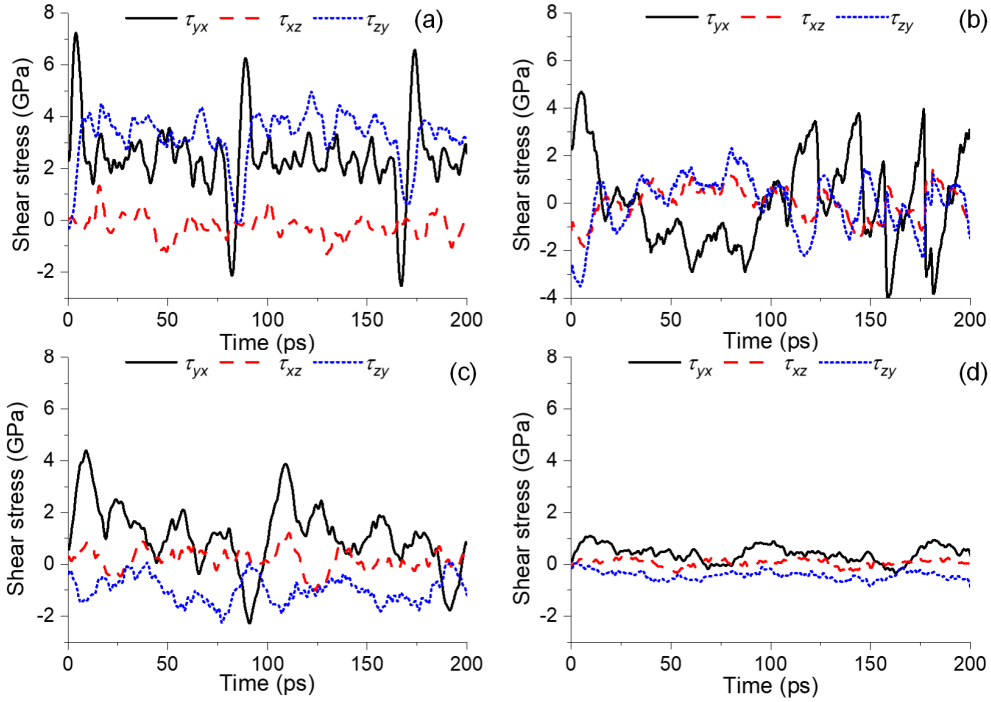

Figure 15. Shear stress of bitumen molecules on the (**a**) calcite, (**b**) anorthite, (**c**) augite, and (**d**) albite mineral substrates under shearing forces.

3.5. Relationship between Macrorheological Characteristics and Nanomolecular Interactions

The macrorheological behavior of mastics in contact with different mineral aggregates is the synthetic result of the bitumen–mineral interaction and the bitumen nanostructural evolution under shearing forces. The linear rheological characteristics of mastic may be closely related to the equilibrated bitumen–mineral nanostructure. The bitumen–calcite system simultaneously contains a stable bitumen colloidal structure in the bulk and an adsorbed polar molecular layer on the mineral surface at 298 K, as seen in Figure 12, resulting in the high complex modulus of the mastic on the limestone at a low temperature. In contrast, in the bitumen–augite and bitumen–albite systems, the Mg^{2+} and Na^{+} diffuse into the bitumen and adsorb the resins from the bitumen's colloid, leading to the asphaltene self-aggregation and the separation from the resin. The augite and albite in the basalt impair the bitumen–basalt interaction, despite the similar strong interaction of the anorthite with bitumen to the calcite. Consequently, the complex modulus of the mastic on the basalt was slightly lower than that on the limestone, as shown in Figure 6. When the temperature rises, the bitumen colloidal structure in the bitumen–calcite system gradually collapses and decreases the macro-modulus, whereas the dispersed metal ions in the bitumen constrain the bitumen molecules and strengthen the modulus. This explains the modulus of the mastic on the basalt exceeding that of the mastic on the limestone.

The nanostructural evolution of the bitumen–mineral systems could explain the non-linear rheological response of the mastic on the mineral aggregates from a fundamental molecular perspective, as seen in Figure 16. The colloidal nanostructure and adsorbed layer in the bitumen–calcite system are dragged and provide a strong resistance to shear

displacement, consequently resulting in a high initial and failure modulus at a macroscale. In contrast, in the bitumen–augite and bitumen–albite systems, the resin is entangled by the metal ions from the minerals and separated from the asphaltene self-aggregates. Under the substrate's shear deformation, the metal ions dispersed in the resin with a small steric hindrance are readily relaxed without the destruction and reconstruction of the asphaltene self-aggregates. Therefore, the bitumen–augite and bitumen–albite systems have relatively little resistance to shear deformation, showing the low failure modulus of mastic on the mineral aggregates. The intermolecular interaction and nanostructural evolution of the bitumen–mineral interface provide a fundamental understanding of the macrorheology of mastics on mineral aggregates.

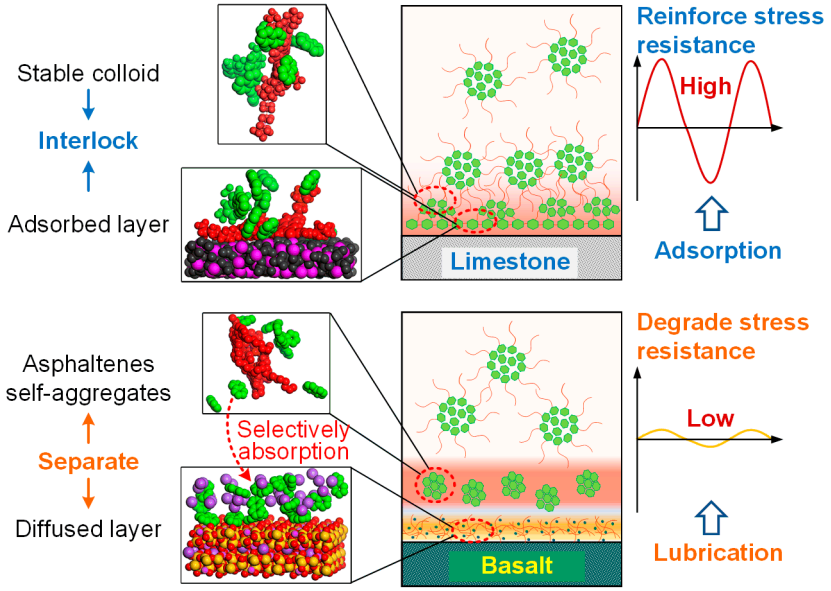

Figure 16. Schematic of the relationship between the macrorheological characteristics and nanomolecular interaction of mastic in contact with the limestone and basalt.

4. Conclusions and Summary

Real asphalt mixtures are fabricated by mixing asphalt mastics and mineral aggregates in the field. The rheological characteristics of mastics attached to mineral aggregates can allow for the more accurate characterization of their rheology than those on steel plates. This study investigated the effects of aggregates on the rheological properties of mastics and explored their fundamental mechanisms using molecular dynamics. The linear and nonlinear rheological properties of the mastics with various filler–bitumen ratios on the different aggregates were compared with that on the steel plate. The intermolecular interactions and nanomechanical characteristics of the bitumen–mineral systems were investigated to explain the influence of the aggregates at a molecular level. The results and analysis led to the following observations:

- The mineral aggregates increased the modulus of the mastics but decreased their phase angles, thereby strengthening the stiffness and toughness of the mastics compared with the mastic on the steel plate.
- The mastic on the limestone substrate had a higher modulus but a lower phase angle than that on the basalt substrate within the linear region at a temperature below 50 °C. The mastic on limestone had a higher modulus than that on basalt, and its ratio reached up to 1.18. This was attributed to the coexistence of the adsorbed bitumen layer and internal colloidal nanostructure in the bitumen–calcite system.
- However, the modulus of the mastic on the basalt exceeded that on the limestone, as the temperature was higher than 50 °C, and the maximum ratio reached 2.17. The stable bitumen nanostructure, containing dispersed metal ions in the bitumen–

augite and bitumen–albite systems at high temperatures, was responsible for the high modulus on the basalt.

- The mastic on the limestone substrate had a better nonlinear rheological performance than that on the basalt substrate. The mastic in contact with the limestone had a higher failure strain and failure modulus than that in contact with the basalt, the ratios of which reached up to 1.60 and 1.32, respectively. Sufficient calcite in the limestone increased the stiffness of the mastic, whereas the augite and albite in the basalt impaired the mastic's performance.
- The bitumen–calcite system had a higher shear stress than the bitumen–augite and bitumen–albite systems and presented a stronger resistance to the substrate shear deformation. The ratio of shear stress of the bitumen-calcite to the bitumen-albite reached up to 6.8. The non-bond energy of the bitumen-calcite was 14.15% higher than that of the bitumen-albite. The destruction and reconstruction of the bitumen colloidal structure in the bitumen–calcite system implies abundant work from external shearing, while small resin and diffused metal ions in the bitumen–augite and bitumen–albite systems form a lubrication layer between the asphaltene self-aggregates and mineral substrates and hardly constrain substrate shearing.
- The chemistry or mineral composition makes an essential contribution to the adhesion and interaction of the mastic–aggregate interface. Considering the influence of mineral aggregates on the rheology of mastic and bitumen is significant for the accurate characterization and prediction of the macroperformance of asphaltic paving material in the field.

The rheological properties of various bitumen-mineral combinations will be investigated for wide temperature, frequency, stress, and strain amplitude ranges. Additional rheological characterization parameters and accurately predicted models of bitumen and mastic on the mineral aggregates will be studied in further work.

Author Contributions: Conceptualization and manuscript writing, Z.L.; measurement, H.W. (Haipeng Wang); methodology and data analysis, X.G.; visualization and review, P.C., language revision, H.W (Hongrui Wei). All authors have read and agreed to the published version of the manuscript.

Funding: This work was supported by the National Natural Science Foundation of China (grant number 52108410), the China Postdoctoral Science Foundation (grant numbers 2022T150432 and 2021M702260), and the Sichuan Transportation Science and Technology Project (grant number 2021-A-14).

Institutional Review Board Statement: Not applicable.

Informed Consent Statement: Not applicable.

Data Availability Statement: Data is contained within the article.

Conflicts of Interest: The authors declare no conflict of interest.

References

1. Anderson, D. *Guidelines on the Use of Baghouse Fines*; National Asphalt Paving Association: Greenbelt, MD, USA, 1987.
2. Craus, J.; Ishai, I.; Sides, A. Some Physiochemical Aspects of the Effect and Role of the Filler in Bituminous Paving Mixtures. *J. Assoc. Asph. Paving Technol.* **1978**, *47*, 558–588.
3. Buttlar, W.G.; Bozkurt, D.; Al-Khateeb, G.G.; Waldhoff, A.S. Understanding Asphalt Mastic Behavior through Micromechanics. *Transp. Res. Rec. J. Transp. Res. Board* **1999**, *1681*, 157–169. [CrossRef]
4. Deng, Y.; Luo, X.; Wang, H. Backcalculation of damage density of in-service asphalt pavements using artificial intelligence-based finite element model updating. *Fatigue Fract. Eng. Mater. Struct.* **2022**, *45*, 671–686. [CrossRef]
5. Ma, X.; Quan, W.; Dong, Z.; Dong, Y.; Si, C. Dynamic response analysis of vehicle and asphalt pavement coupled system with the excitation of road surface unevenness. *Appl. Math. Model.* **2022**, *104*, 421–438. [CrossRef]
6. Deng, Y.; Shi, X.; Kou, Y.; Chen, J.; Shi, Q. Optimized design of asphalt concrete pavement containing phase change materials based on rutting performance. *J. Clean. Prod.* **2022**, *380*, 134787. [CrossRef]
7. Deng, Y.; Shi, X. An Accurate, Reproducible and Robust Model to Predict the Rutting of Asphalt Pavement: Neural Networks Coupled with Particle Swarm Optimization. *IEEE Trans. Intell. Transp. Syst.* **2022**, *23*, 22063–22072. [CrossRef]
8. Delaporte, B.; DiBenedetto, H.; Chevrot, P.; Gauthier, G. Linear Viscoelastic Properties of Bituminous Materials: From Binders to Mastics. *J. Assoc. Asph. Paving Technol.* **2007**, *76*, 445–494.

9. Liu, Z.; Dong, Z.; Zhou, T.; Cao, L. Water vapor diffusion models in asphalt mortar considering adsorption and capillary condensation. *Constr. Build. Mater.* **2021**, *308*, 125049. [CrossRef]
10. Rigden, P.J. The use of fillers in bituminous road surfacings. A study of filler-binder systems in relation to filler characteristics. *J. Soc. Chem. Ind.* **1947**, *66*, 299–309. [CrossRef]
11. Anderson, D.; Bahia, H.; Dongre, R. Rheological Properties of Mineral Filler-Asphalt Mastics and Its Importance to Pavement Performance. In *Effects of Aggregates and Mineral Fillers on Asphalt Mixture Performance*; ASTM International: West Conshohocken, PA, USA, 1992; pp. 131–153.
12. Chen, J.-S. Rheological Properties of Asphalt-Mineral Filler Mastics. *J. Mater. Concr. Struct. Pavements* **1997**, *36*, 269–277. [CrossRef]
13. Cooley, L.A.; Stroup-Gardinder, M.; Brown, E.R.; Hanson, D.I.; Fletcher, M.O. Characterization of Asphalt-Filler Mortars with Superpave Binder Tests. In Proceedings of the Journal of the Association of Asphalt Paving Technologists, Boston, MA, USA, 16–18 March 1998; Volume 67.
14. Buttlar, W.G.; Roque, R. Evaluation of Empirical and Theoretical Models to Determine Asphalt Mixture Stiffnesses at Low Temperatures. In Proceedings of the 1996 Conference of the Association of Asphalt Paving Technologies, Baltimore, MD, USA, 18–20 March 1996; Volume 65, pp. 99–141.
15. Shashidhar, N.; Romero, P. Factors Affecting the Stiffening Potential of Mineral Fillers. *Transp. Res. Rec.* **1998**, *1638*, 94–100. [CrossRef]
16. Shashidhar, N.; Shenoy, A. On using micromechanical models to describe dynamic mechanical behavior of asphalt mastics. *Mech. Mater.* **2002**, *34*, 657–669. [CrossRef]
17. Kim, Y.-R.; Little, D.N. Linear Viscoelastic Analysis of Asphalt Mastics. *J. Mater. Civ. Eng.* **2004**, *16*, 122–132. [CrossRef]
18. Druta, C. A Micromechanical Approach for Predicting the Complex Shear Modulus and Accumulated Shear Strain of Asphalt Mixtures from Binder and Mastics. Ph.D. Dissertation, Louisiana State University, Baton Rouge, LA, USA, 2006. [CrossRef]
19. Kumlai, S.; Jitsangiam, P.; Nikraz, H. Assessments of moisture damage resistance of asphalt concrete mixtures and asphalt mastic with various mineral fillers. *Transp. Eng.* **2022**, *7*, 100106. [CrossRef]
20. Xu, O.; Xiang, S.; Yang, X.; Liu, Y. Estimation of the surface free energy and moisture susceptibility of asphalt mastic and aggregate system containing salt storage additive. *Constr. Build. Mater.* **2022**, *318*, 125814. [CrossRef]
21. Scholz, T.V.; Brown, S.F. Rheological Characteristics of Bitumen in Contact with Mineral Aggregate (with Discussion). In Proceedings of the Journal of the Association of Asphalt Paving Technologists, Baltimore, MD, USA, 18–20 March 1996; pp. 357–384.
22. Huang, S.-C.; Branthaver, J.F.; Robertson, R.E.; Kim, S.-S. Effect of Film Thickness on the Rheological Properties of Asphalts in Contact with Aggregate Surface. *Transp. Res. Rec.* **1998**, *1638*, 31–39. [CrossRef]
23. Cho, D.-W.; Bahia, H.U. Effects of Aggregate Surface and Water on Rheology of Asphalt Films. *Transp. Res. Rec.* **2007**, *1998*, 10–17. [CrossRef]
24. E, G.; Zhang, J.; Shen, Q.; Ji, P.; Wang, J.; Xiao, Y. Influence of Filler Type and Rheological Properties of Asphalt Mastic on the Asphalt Mastic–Aggregate Interaction. *Materials* **2023**, *16*, 574. [CrossRef]
25. Huang, Q.; Qian, Z.; Hu, J.; Zheng, D.; Chen, L.; Zhang, M.; Yu, J. Investigation on the properties of aggregate-mastic interfacial transition zones (ITZs) in asphalt mixture containing recycled concrete aggregate. *Constr. Build. Mater.* **2021**, *269*, 121257. [CrossRef]
26. Wang, P.; Zhai, F.; Dong, Z.-J.; Wang, L.-Z.; Liao, J.-P.; Li, G.-R. Micromorphology of Asphalt Modified by Polymer and Carbon Nanotubes through Molecular Dynamics Simulation and Experiments: Role of Strengthened Interfacial Interactions. *Energy Fuels* **2018**, *32*, 1179–1187. [CrossRef]
27. Xu, M.; Yi, J.; Feng, D.; Huang, Y.; Wang, D. Analysis of Adhesive Characteristics of Asphalt Based on Atomic Force Microscopy and Molecular Dynamics Simulation. *ACS Appl. Mater. Interfaces* **2016**, *8*, 12393–12403. [CrossRef]
28. Dong, Z.; Liu, Z.; Wang, P.; Gong, X. Nanostructure characterization of asphalt-aggregate interface through molecular dynamics simulation and atomic force microscopy. *Fuel* **2017**, *189*, 155–163. [CrossRef]
29. Liu, Z.; Cao, L.; Zhou, T.; Dong, Z. Multiscale Investigation of Moisture-Induced Structural Evolution in Asphalt–Aggregate Interfaces and Analysis of the Relevant Chemical Relationship Using Atomic Force Microscopy and Molecular Dynamics. *Energy Fuels* **2020**, *34*, 4006–4016. [CrossRef]
30. Li, C.; Ma, F.; Fu, Z.; Dai, J.; Wen, Y.; Shi, K. Investigation of the solution effects on asphalt binder and mastic through molecular dynamics simulations. *Constr. Build. Mater.* **2022**, *345*, 128314. [CrossRef]
31. MTPRC. *Technical Specifications for Construction of Highway Asphalt Pavements (JTG F40-2004)*; China Communications Press: Beijing, China, 2004.
32. Zhang, L.; Greenfield, M.L. Molecular Orientation in Model Asphalts Using Molecular Simulation. *Energy Fuels* **2007**, *21*, 1102–1111. [CrossRef]
33. Atkins, P.; de Paula, J. *Physical Chemistry for the Life Sciences*, 2nd ed.; Oxford University Press: New York, NY, USA, 2015; ISBN 978-0-19-956428-6.